

# Non-Parametric Deformable Registration of High Angular Resolution Diffusion Data Using Diffusion Profile Statistics

P-T. YAP<sup>1</sup>, Y. CHEN<sup>1</sup>, H. AN<sup>1</sup>, J. H. GILMORE<sup>2</sup>, W. LIN<sup>1</sup>, AND D. SHEN<sup>1</sup>

<sup>1</sup>DEPARTMENT OF RADIOLOGY, UNIVERSITY OF NORTH CAROLINA, CHAPEL HILL, NORTH CAROLINA, UNITED STATES, <sup>2</sup>DEPARTMENT OF PSYCHIATRY, UNIVERSITY OF NORTH CAROLINA, CHAPEL HILL, NORTH CAROLINA, UNITED STATES

**INTRODUCTION:** The shortcoming of Diffusion Tensor Imaging (DTI) in resolving intra-voxel multiple fiber crossings has prompted great interest in developing more sophisticated models. Specifically, Tuch et al. [1] introduced a High Angular Resolution Diffusion Imaging (HARDI) method, suggesting that the apparent diffusion coefficients could be evaluated along many different directions without fitting a global function to the data. The outcome is a diffusion profile consisting of an angular distribution of apparent diffusivities. In this abstract, we propose a full-brain multi-scale feature-based deformable registration algorithm based on the statistics of the diffusion profile of HARDI data. Besides the advantage of avoiding any predetermined models which may not necessarily fit the data, our method registers the diffusion weighted images (DWIs) and allows model fitting after the registration. This essentially means that our method can be utilized as a preprocessing step for a wide assortment of available diffusion models. Our method is also well suited for clinical applications due to its low computational cost – around 5 minutes on a 2.8GHz Linux machine (without algorithm optimization) to register a pair of images of typical size 128 x 128 x 80. The main idea involves extraction of statistical features directly from the diffusion profile, which includes mean diffusivity, diffusion anisotropy, regional diffusion statistics, and statistic-map-based edges. For each voxel, we group all these features into a single feature vector as its structural signature for correspondence matching. We employ a hierarchical matching scheme where initially only voxels with the most distinctive feature vectors are allowed to guide the registration, mitigating matching error caused by voxels with less distinctive feature vectors. Upon obtaining a coarse but robust alignment of the images, we allow an increasing number of voxels with progressively decreasing saliency to participate in refining the registration. To cater for structural patterns of different scales, registration is performed on an image pyramid of different scales, starting from a coarse scale and ending with a fine scale.

**METHODS: [Features]** Using the Stejskal-Tanner expression [2], the signal attenuation value  $E(\mathbf{g})$  on a  $q$ -space sphere defined by diffusion weighting factor  $b$  in the diffusion direction specified by unit vector  $\mathbf{g}$  can be express as:  $E(\mathbf{g})=\exp(-bD(\mathbf{g}))$ . Diffusion profile  $D(\mathbf{g})$  has a complex structure in voxels with orientation heterogeneity [3]. We leverage the wealth of information contained in the diffusion profile by extracting relevant statistics for guidance of registration. 1) **Mean Diffusivity:** Defined as the mean of the diffusivity profile,  $\langle D(\mathbf{g}) \rangle_{\mathbf{g}}$ , where  $\langle D(\mathbf{g}) \rangle$  denotes averaging over  $\mathbf{g}$ , 2) **Diffusion Anisotropy:** The deviation of the diffusivity profile from its isotropic equivalent with the same mean diffusivity,  $\sqrt{\langle (D(\mathbf{g}) - \langle D(\mathbf{g}) \rangle_{\mathbf{g}})^2 \rangle_{\mathbf{g}}}$ , 3) **Regional Mean Diffusivity:** Defined as the mean diffusivity of a local spatial region  $\langle \langle D_z(\mathbf{g}) \rangle_z \rangle_{\mathbf{g}}$ , where  $D_z(\mathbf{g})$  is the apparent diffusion diffusivity at location  $\mathbf{z}$  in the neighborhood  $N(\mathbf{x})$  of  $\mathbf{x}$ . 4) **Regional Diffusion Variance:** Measures the deviation of the diffusivities of the surrounding voxels from the regional mean diffusivity,  $\sqrt{\langle \langle (D_z(\mathbf{g}) - \langle \langle D_z(\mathbf{g}) \rangle_z \rangle_{\mathbf{g}})^2 \rangle_z \rangle_{\mathbf{g}}}$ . 5) **Edges of Mean Diffusivity and Diffusion Anisotropy Maps:** Edge maps computed from the statistical maps by applying a 3D Canny edge detector - important for characterizing and ensuring proper alignment of ventricular and white-matter boundaries. **[Correspondence matching]** The above-mentioned features are collected into a feature vector for each voxel as its structural signature for correspondence matching. The following strategies are employed for robust matching: 1) **Automatic hierarchical landmark selection:** A salient-feature priority scheme where automatic landmarks are progressively selected in decreasing saliency (according to the feature vector distinctiveness of a voxel) to participate in guiding the registration, 2) **Soft-correspondence:** where we allow all possible candidate correspondence points (with sufficient feature vector similarity to a current landmark point) to be given respective weights, so that in the end we can come to a deformation target location based on a final, more informed, weighted decision. 3) **TPS-Interpolation:** A hierarchical thin-plate spline (TPS) [4] interpolation strategy, where we ensure well-behaving transformation to properly preserve biologically meaningful topology, first for the prominent major structures and then for the finer minor structures. More description of these strategies can be found in [5]. **[Retransformation]** Unlike the diffusion tensors, reorientation alone is not meaningful for HARDI data which can resolve multiple fiber directions [6]. In our method, we retransform the DWIs by rotating the gradient directions using  $\mathbf{g}' = \mathbf{F}\mathbf{g} / \|\mathbf{F}\mathbf{g}\|$ , where  $\mathbf{F}$  is a local affine transformation estimated from the deformation field. This essentially gives each voxel a new set of gradient directions, which can be utilized for estimation of a wide variety of diffusion models after registration.

**MATERIALS:** 6 adult subjects were scanned using an EPI sequence with  $b$  values 1000s/mm<sup>2</sup> and 3000s/mm<sup>2</sup> applied in 120 non-collinear directions (NEX=1). 80 contiguous slices with slice thickness of 2mm covered a field of view (FOV) of 256 x 256mm<sup>2</sup> with an isotropic voxel size of 2mm.

**RESULTS: [Registration Accuracy]** Selecting one image (from the set of images acquired with  $b=1000\text{s/mm}^2$ ) as the template, we registered the other 5 images onto the template and measured the registration consistency by computing the normalized scalar products of the diffusion anisotropy maps of the aligned images with respect to that of the mean image generated by the aligned images. Our method gives a high average value of 0.92 (the highest possible value is 1), and is significantly better compared to affine registration (paired  $t$ -test,  $p=0.016$ ). Moreover, compared with the deformation field estimated by a recently introduced state-of-the-art DTI registration algorithm called F-TIMER [5], our method, despite its current unoptimized state, also yields 1% performance gain. With the addition of more features, our method can potentially outperform F-TIMER more significantly. Fig. 2 demonstrates that the outcome produced by the proposed method matches the structures of the template more closely than anisotropy map based affine registration. **[Noise Robustness]** We evaluated the performance of our algorithm with respect to noise by performing the same registration process on the set of images acquired using  $b=3000\text{s/mm}^2$ . Despite the decreased SNR, registration performance of our method, as measured by the normalized scalar product, does not show statistically significant degradation (paired  $t$ -test,  $p=0.55$ ).

**CONCLUSION:** We have proposed a fast multi-scale deformable registration algorithm for HARDI. Our method does not impose any model and can be utilized as a spatial normalization preprocessing step for a wide assortment of models.

**REFERENCES:** [1] Tuch et al., ISMRM 1999. [2] Stejskal and Tanner, J. Chem Phys, 1965. [3] Tuch et al., MRM, 2002. [4] Bookstein et al, 1989. [5] Yap et al., MICCAI, 2009. [6] Barmpoutis et al., MICCAI, 2007.

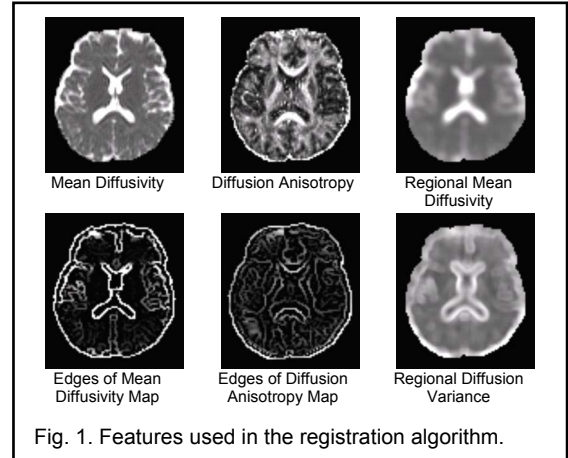


Fig. 1. Features used in the registration algorithm.

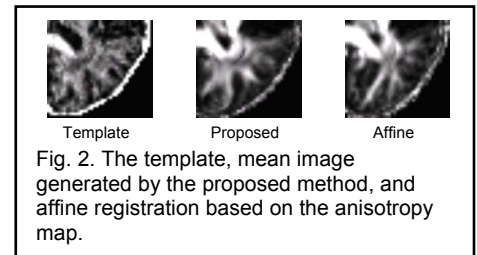


Fig. 2. The template, mean image generated by the proposed method, and affine registration based on the anisotropy map.